https://doi.org/10.48048/tis.2022.493

Callistemon viminalis Leaf Extract Mediated Biosynthesis of Ag, rGO-Ag-ZnO Nanomaterials for Catalytic PEM Fuel Cell Application

Pankaj Kumar Jha[1], Chamorn Chawengkijwanich[2], Kuaanan Techato[3], Warakorn Limbut[4] and Montri Luengchavanon[5,*]

[1]*Sustainable Energy Management Program, Faculty of Environmental Management, Prince of Songkla University, Songkhla 90110, Thailand*
[2]*Environmental Nanotechnology Team, National Nanotechnology Center, National Science and Technology Development Agency, Thailand Science Park, Pathum Thani 12120, Thailand*
[3]*Environmental Assessment and Technology for Hazardous Waste Management Research Center, Faculty of Environmental Management, Prince of Songkla University, Songkhla 90110, Thailand*
[4]*Division of Health and Applied Sciences, Thailand Center of Excellence for Innovation in Chemistry, Center of Excellence for Trace Analysis and Biosensor, Faculty of Science, Prince of Songkla University, Songkhla 90110, Thailand*
[5]*Sustainable Energy Management Program, Wind Energy and Energy Storage Systems Centre, Faculty of Environmental Management, Center of Excellence in Metal and Materials Engineering, Faculty of Engineering, Prince of Songkla University, Songkhla 90110, Thailand*

([*]Corresponding author's e-mail: montri.su@psu.ac.th)

Received: 13 November 2021, Revised: 28 December 2021, Accepted: 13 January 2022

Abstract

Cost-effective manufacture of hydrogen proton exchange membrane fuel cells (PEM-fuel cells) is of much interest to concerned researchers. Platinum metal has already shown good performance in the PEM fuel cell, yet its high cost means that it is not affordable to all nations. This paper identifies ways to reduce the cost by replacing platinum-based PEM fuel cells with synthesised eco-friendly silver (Ag) nanoparticles and reducing graphene oxide coated silver composited zinc oxide (rGO/Ag-ZnO) nanomaterials. Ag nanoparticles and reduced graphene oxide coated silver composited zinc oxide nanomaterials were synthesised using *Callistemon viminalis* leaf extract. PEM fuel cell modification was achieved using newly biosynthesised nanomaterials, while power density was compared with commercial platinum metal-based PEM fuel cells. The present study shows that modified PEM fuel cells can replace commercial platinum-based PEM fuel cells for cost-effective hydrogen proton exchange membrane fuel cells.

Keywords: *Callistemon viminalis* leaf, Metal Nanoparticles, Hydrogen conversion, Power Density, Green Energy

Introduction

In the current global context, the growing population is exercising a greater demand for energy in order to conduct daily household activities, while there is also a need to focus on alternative energy forms [1]. Alternative energy production from proton exchange membrane fuel cells (PEM) is of great interest at present because hydrogen energy can be converted into electricity by transferring hydrogen ions (H^+) through electrodes at a high-power density [2-3]. Hydrogen production can be achieved using an electrolyser, in which high pressure is applied to generate hydrogen ions [4]. Various approaches have been used to produce hydrogen ions, including hydrocarbon reforming methods, biomass methods and water splitting methods. Biomass and hydrocarbon reforming methods are high risk and toxic to the environment [5]. Water splitting methods are the best to overcome challenges to the mass production of hydrogen energy through the design of modified catalysts [6]. An emerging topic based on nanomaterials for hydrogen energy harvesting is gaining greater attention due to their shape, size, dimensions, pH dependence, crystallinity, and band gap properties [7]. Eco-friendly catalysts are required to limit environmental pollution and harvest clean energy from water splitting methods [8].

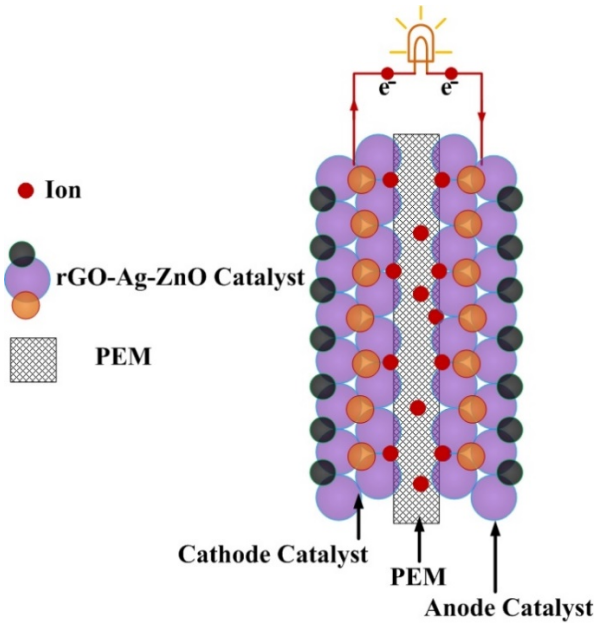

Figure 1 Overview of PEM fuel cell.

As shown in **Figure 1**, PEM fuel cells have ionic transport in which the electrode has a vital role in the current collection. The challenge of this system is the high cost of platinum metal which is used as an electrode. Cost analysis indicates that there is efficient power output generated from PEM fuel cells which directly affects national economies due to the high cost of conventional platinum metal-based PEM fuel cells [9]. Recently, hydrogen technology as a part of sustainable energy management has seen increased demand and is recognised for its future importance. Yet managing the technological challenges of PEM fuel cells is still required [10]. To design a cheaper PEM fuel cell electrode, this research involved coating biosynthesised silver nanoparticles and reducing graphene oxide silver composited zinc oxide nanomaterials on an aluminium metal electrode.

Materials and methods

Sodium hydroxide, silver nitrate and zinc hexahydrate were purchased from Loba Chemie Pvt. Ltd., Thailand. Graphene oxide concentration solution was purchased from Graphenea, Spain. PEM fuel cell stack was purchased from Horizon fuel cell, Thailand. Aluminium (Al) plates of 0.5 mm thickness were bought and cut into 2.5×2.5 cm^2 square shapes, similar to a commercial PEM fuel cell stack. *Callistemon viminalis* plant leaf was taken from Hat Yai Agricultural Park, located in Hat Yai, Songkhla, Thailand.

Thirty g of *Callistemon viminalis* leaf was washed with deionized water and cut into small pieces. Small leaf pieces were mixed with 250 mL of deionized water and boiled at 60 ºC for 20 min with a magnetic stirrer. After boiling, the leaf extract was filtered with Whatman no.1 filter paper and cooled at room temperature [11].

Two g of zinc nitrate hexahydrate was mixed with 100 mL of deionized water and shaken well to mix properly. One-hundred mL of *Callistemon viminalis* leaf extract, 1 mM silver nitrate solution, and 10 mL of graphene oxide concentration were mixed in a zinc oxide solution. One N sodium hydroxide solution was added drop-by-drop to maintain the solution at pH 10. The solution was then stirred with a magnetic stirrer bar at 60 ºC until a dark brown colour was obtained.

One mmol of silver nitrate solution in 100 mL was mixed with 100 mL of *Callistemon viminalis* leaf extract. One N sodium hydroxide solution was added drop-by-drop to maintain the solution at pH 10. The solution was then stirred with a magnetic stirrer bar at 60 ºC until a reddish-brown colour was obtained, as shown in **Figure 2** [12].

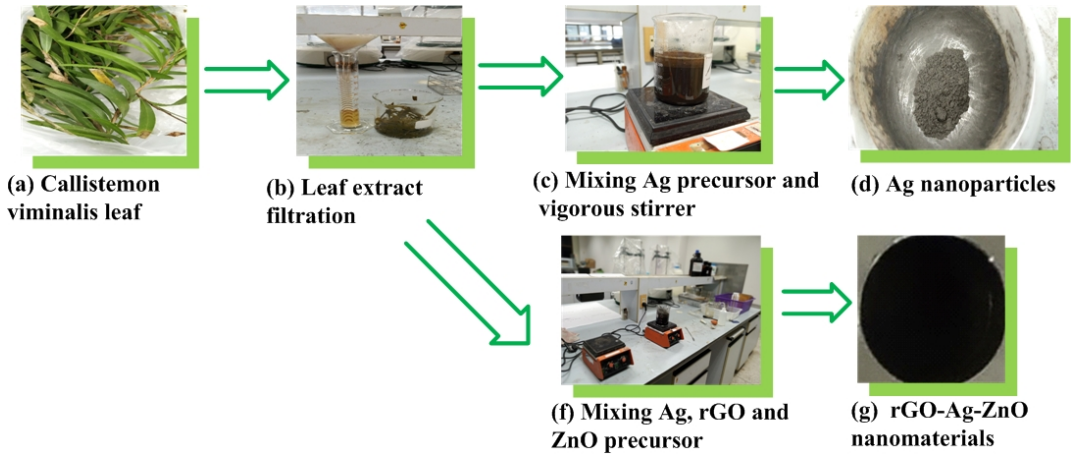

Figure 2 Biosynthesis of Ag nanoparticles and rGO/Ag-ZnO nanomaterials.

Aluminium plate electrodes were coated with Ag nanoparticles. Power density was calculated using a flow rate of 0.3 L/min of hydrogen gas and 0.5 L/min of oxygen gas into the PEM fuel cell stack. Similarly, aluminium plate electrodes were also coated with r-GO/Ag-ZnO nanomaterials. Power density was calculated using a flow rate of 0.3 L per min of hydrogen gas and 0.5 L per min of oxygen gas into the PEM fuel cell stack. The power density was calculated from different modified metal plate electrodes compared with the power density of commercial proton exchange membrane fuel cell at a similar flow rate of 0.3 L per min of hydrogen gas and 0.5 L per min of oxygen gas [13].

Ultraviolet visible analysis was conducted at wavelengths from 200 to 800 nm using UV-Visible spectroscopy model number DR 6000 (Envi Science company limited). The surface morphology and elemental compositions were examined using FE-SEM Apreo-EDX. TEM analysis was performed using an electron probe X-ray micro analyser JXA 8900R. The functional group attached on the nanoparticle surface was analysed by ATR and KBr pallet technique using a Fourier Transform Infrared Spectrometer (VERTEX 70, Bruker, Bremen, Germany). Surface roughness was analysed by atomic force microscopy AFM-flex. XRD Empyrean was used to identify crystallinity and phase identification. Electrochemical impedance spectroscopy (EIS) was used for analysis by using a Potentiostat/Galvanostat (PGSTAT302N, Metrohm, Autolab, Netherlands). Power density analysis was performed using Solar Power Modular (Solar PV analyser).

Results and discussion

Ultraviolet visible absorbance

Ultraviolet visible absorption for Ag nanoparticle appears at a wavelength of 424 nm. UV-Vis absorption for r-GO/Ag-ZnO nanomaterials showed at 345 nm wavelength, confirming the desorption of the oxygen attached to the graphene layers, as shown in **Figure 3** [14].

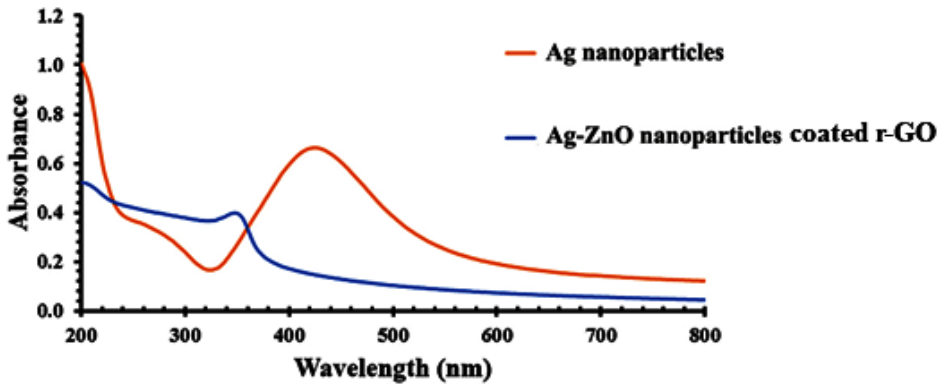

Figure 3 UV-Visible analysis of Ag nanoparticles and r-GO/Ag-ZnO nanomaterials.

Field emission scanning electron microscopy analysis

Field emission scanning electron microscopy analysis shows an average size of 28 nm for Ag nanoparticles, as shown in **Figure 4**(**b**). **Figure 4**(**a**) shows reduced graphene oxide coated on silver (Ag) composited zinc oxide nanomaterials under a 1-micron metre scale. Field emission scanning electron microscope analysis shows a 13-micron metre average pinhole gap between each Ag nanoparticle under a 100-micron metre scale (**Figure 5**(**a**)), and 35 nm under a 500 nm scale in Ag coated on an aluminium plate (**Figure 5**(**c**)). Similarly, the average thickness of Ag nanoparticles on the aluminium plate show a 131-micron metre as shown in **Figure 5**(**b**) [15].

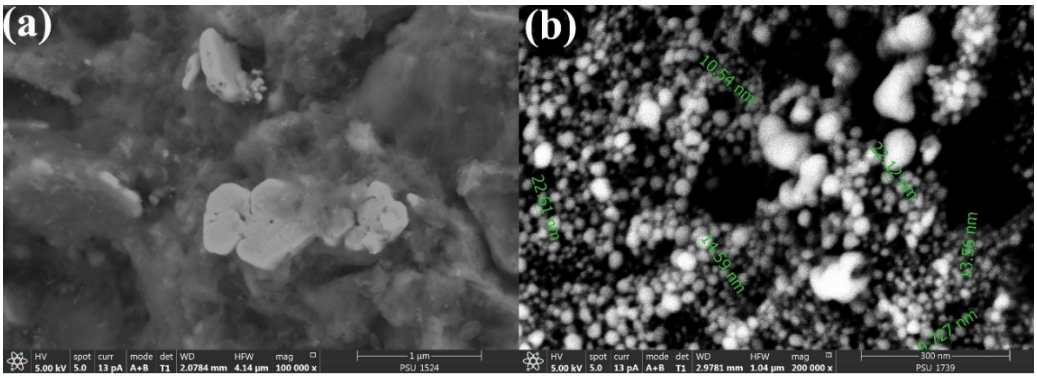

Figure 4 FE-SEM analysis of (a) rGO/Ag-ZnO nanomaterials and (b) Ag nanoparticles.

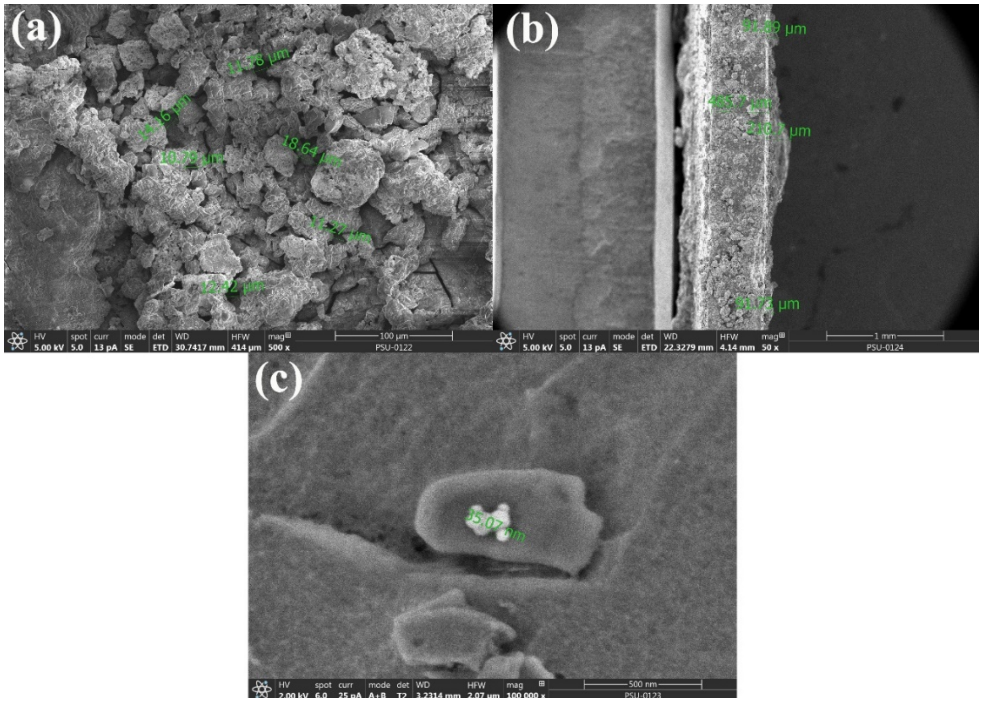

Figure 5 FE-SEM analysis of (a) Ag nanomaterials coated on an aluminium plate, (b) cross sectional view, (c) pinhole.

Atomic force microscopy analysis

The surface of the cathode and anode of PEM fuel cell can affect hydrogen and oxygen gases. The nanoparticle materials coated in electrode forms the porosity that increase surface area. Nanoparticle coatings on the electrode also exhibited very small roughness. The average root mean square (sq.) of Ag nanoparticles roughness on Al plate shows 1053.7 picometre (pm) on a 1-micron metre scale, as shown in **Figure 6** [16].

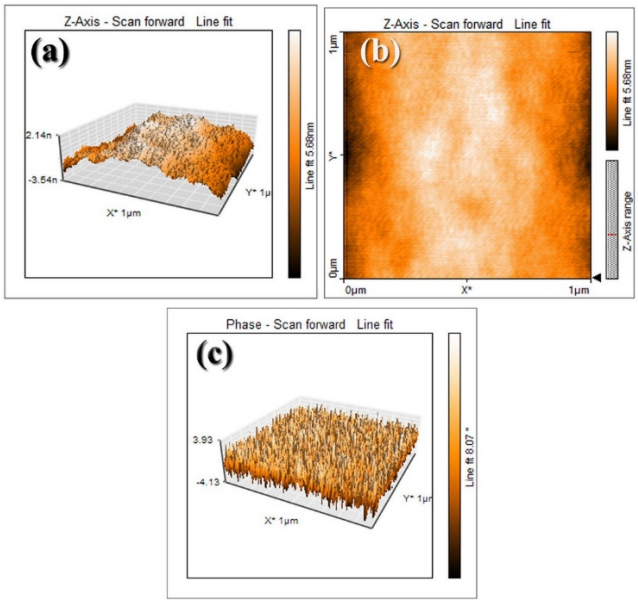

Figure 6 AFM analysis of Ag nanoparticles coated on an aluminium plate that performed surface area (a) Z-axis scan forward performed by 3 dimension, (b) Z-axis scan forward performed by 2 dimension (c) phase-scan forward performed by 3 dimension.

Energy dispersive X-ray analysis

rGO/Ag-ZnO nanomaterials can increase the electrochemical reaction in the PEM fuel cell. Energy dispersive x-ray analysis confirmed the ratio of the mixture that was coated on the electrode. The elemental composition of the rGO/Ag-ZnO nanomaterials show 17.4 Wt% of carbon (C), 11.4 Wt% of Ag, 42.6 Wt% of zinc (Zn), 24.8 Wt% of oxygen, and 3.8 Wt% of other elements, as shown in **Figure 7** [17].

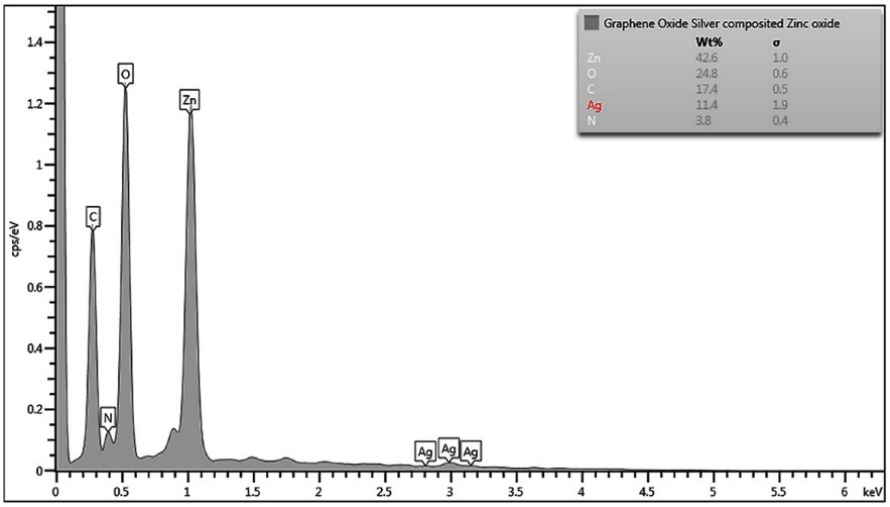

Figure 7 EDX analysis of rGO/Ag-ZnO nanomaterials.

Transmission electron microscopy analysis

The high resolution transmission electron microscopy plane-view image confirms the structure of silver nanoparticles. Transmission electron microscopy analysis shows that the Ag nanoparticles had an average size of 46 nm and a cubic structure. Lattice spacing was 0.25 nm (**Figure 8**(**a**)), and the selected area electron diffraction pattern confirms the formation of silver nanoparticles (**Figure 8**(**b**)) [18].

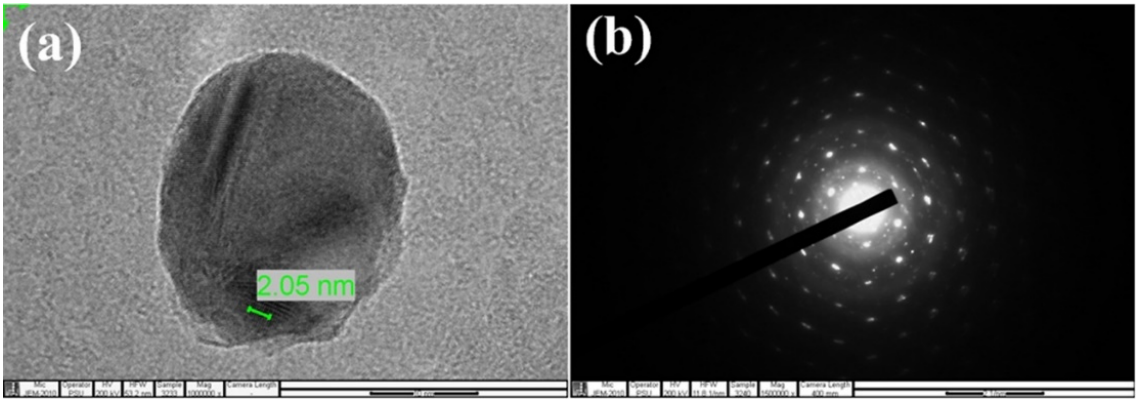

Figure 8 TEM-SAED pattern analysis of Ag nanoparticles (a) Lattice spacing and (b) Selected area electron diffraction pattern.

X-ray diffraction analysis

The x-ray diffraction analysis for Ag nanoparticles shows Muller indices (111) at a diffraction angle of (2Θ) 38º, (200) at 44.20º, (220) at 64.40º, (311) at 77.29º and (222) at 81.25º. Similarly, the percentage of crystallinity was 85.14 % and crystal size was 22 nm. X-ray diffraction analysis shows reduced graphene oxide (r-GO) Muller indices (110) at a diffraction angle of (2Θ) 12.73º, (200) at 18.11º, and (220) at 25.56º. Ag nanoparticles show Muller indices (111) at a diffraction angle of (2Θ) 38º, (200) at 44º, (220) at 64.39º and (311) at 77.40º with a crystal size of 45 nm. Zinc Oxide (ZnO) nanoparticles show Muller indices (100) at a diffraction angle (2Θ) 32º, (002) at 34º and (101) at 36º with a crystal size of 23 nm. Similarly, the percentage of crystallinity shows 60.28 % in rGO/Ag-ZnO nanomaterials (**Figure 9**) [19].

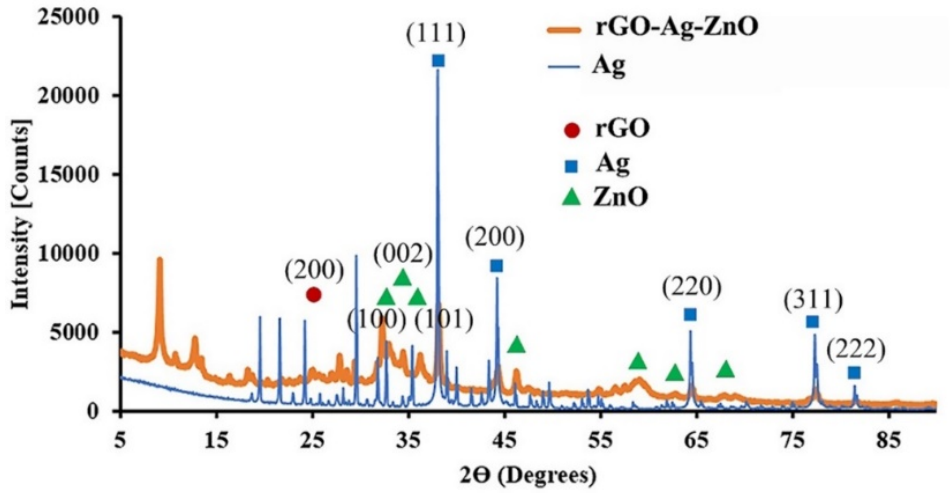

Figure 9 XRD analysis of Ag nanoparticles and rGO/Ag-ZnO nanomaterials.

Fourier transform infrared analysis

Fourier transform infrared analysis confirmed the functional group attached. Ag nanoparticles wavenumber (cm^{-1}) at 3451, 2921, 2852, 1762, 1628, 1383, 1274 and 824 had O-H stretching, C-H stretching, and C-H stretching confirming the functional group attachment C=O, N-H, C-N or C-O, C-N, and O-H, respectively as shown in **Figure 10**(**a**). Similarly, rGO/Ag-ZnO nanomaterials functional groups are attached at wavenumber (cm^{-1}) 519, 620, 820, 1029, 118, 1314, 1587, 2930 and 3323 have C-Br stretching, C=C bending, C-N stretching, C-O stretching, C-N stretching, C-H stretching, and O-H stretching, confirming the functional group attachment halo compound, alkene, amine, secondary alcohol, aromatic amine, cyclic alkene, alkane and carboxylic acid, respectively, as shown in **Figure 10**(**b**) [20].

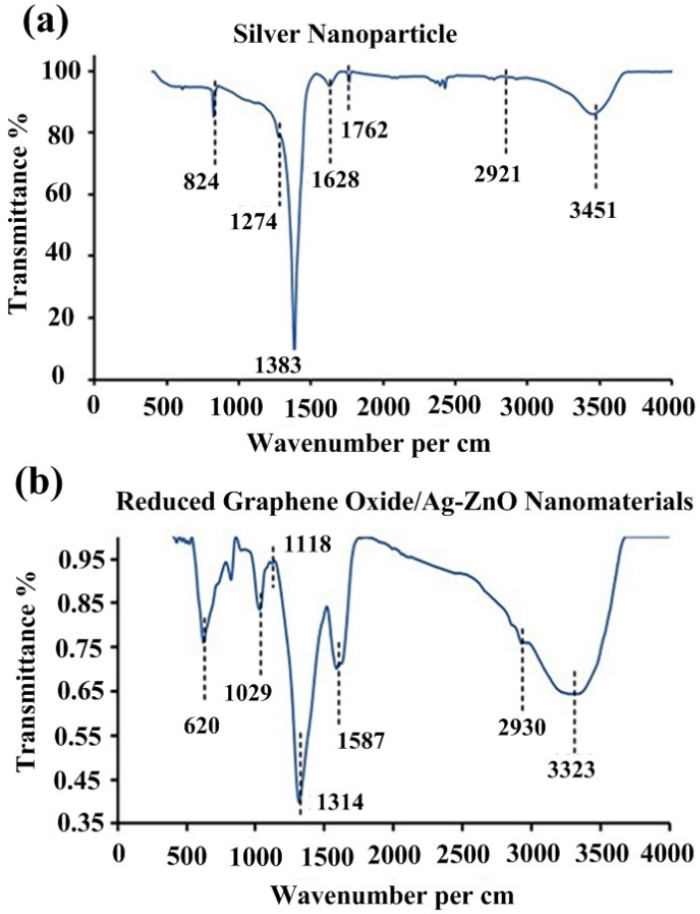

Figure 10 FTIR analysis of (a) Ag nanoparticles and (b) rGO/Ag-ZnO nanomaterials.

Electrochemical impedance spectroscopy analysis

Nyquist plots were used to investigate the electrochemical impedance spectroscopy (EIS) data, as shown in **Figure 11**. Two electrodes represented the typical AC impedance characteristics of a polymer electrolyte membrane (PEM). The high-frequency region provides 2 pieces of information: (a) The real axis intercept shows a combined resistance (Rs) that contains intrinsic resistance of electrode materials, ionic resistance of electrolyte, and contact resistance between the electrode and current collector; and (b) The radius of the semicircle is indicative of the electrode conductivity and charge transfer resistance (Rct) of the electrode materials. The EIS plots represent identical Rs for Ag at around 4.00 Ω, which was larger than that of rGO-Ag-ZnO (2.00 Ω). The fitted value of Rct obtained for Ag and rGO-Ag-ZnO were 160.00 and 75.00 Ω, respectively. The smaller diameter semicircle for rGO-Ag-ZnO than for Ag indicates the low resistance of rGO-Ag-ZnO. The semicircle diameter can approximately indicate the charge-transfer resistance of Rct, while the rGO/C/ZnO electrode shows a smaller Rct than C/ZnO or rGO/ZnO, indicating better electrochemical activity [21]. Additionally, the Nyquist plots of Ag-rGO reveal depressed semicircles at high frequencies compared to rGO, indicating the high electrical conductivity of Ag-rGO achieved by doping Ag onto rGO sheets [22].

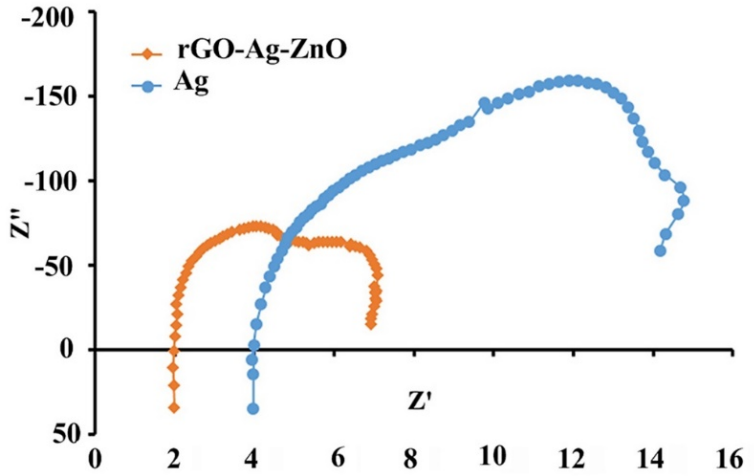

Figure 11 EIS analysis of Ag nanoparticles and rGO/Ag-ZnO nanomaterials.

Power density

Power density analysis indicates commercial PEM fuel cell 0.14 mW/cm^2, Ag nanoparticles coated on an aluminium plate 0.06 mW/cm^2, and rGO/Ag-ZnO nanomaterials coated on an aluminium plate 0.10 mW/Cm^2, as shown in the I-V curve in **Figure 12** [23].

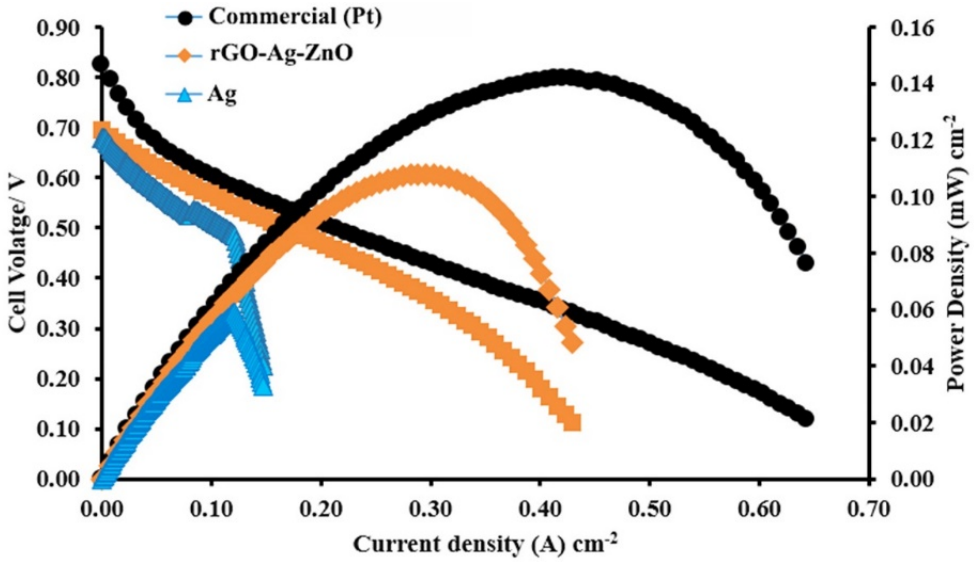

Figure 12 Power density analysis of commercial PEM fuel cell, rGO/Ag-ZnO nanomaterials coated on an aluminium plate, and Ag nanoparticles coated on an aluminium plate.

Environmental economic analysis

Environmental economic analysis shows that a commercial PEM fuel cell can give 100 % electricity production at $156 (USD). Meanwhile, the newly designed PEM fuel cell shows 238.774 % electricity production by Ag NPs coated aluminium electrode after increasing the cost from $28 to $156. Similarly, the rGO/Ag-ZnO NPs coated aluminium electrode after increasing the cost from $30 to $156 shows 371.4256 % electricity production, as shown in **Figure 13**(**b**). This is due to the price variations in the 3 different PEM fuel cells and the percentage of electricity production (**Figure 13**(**a**)) [24].

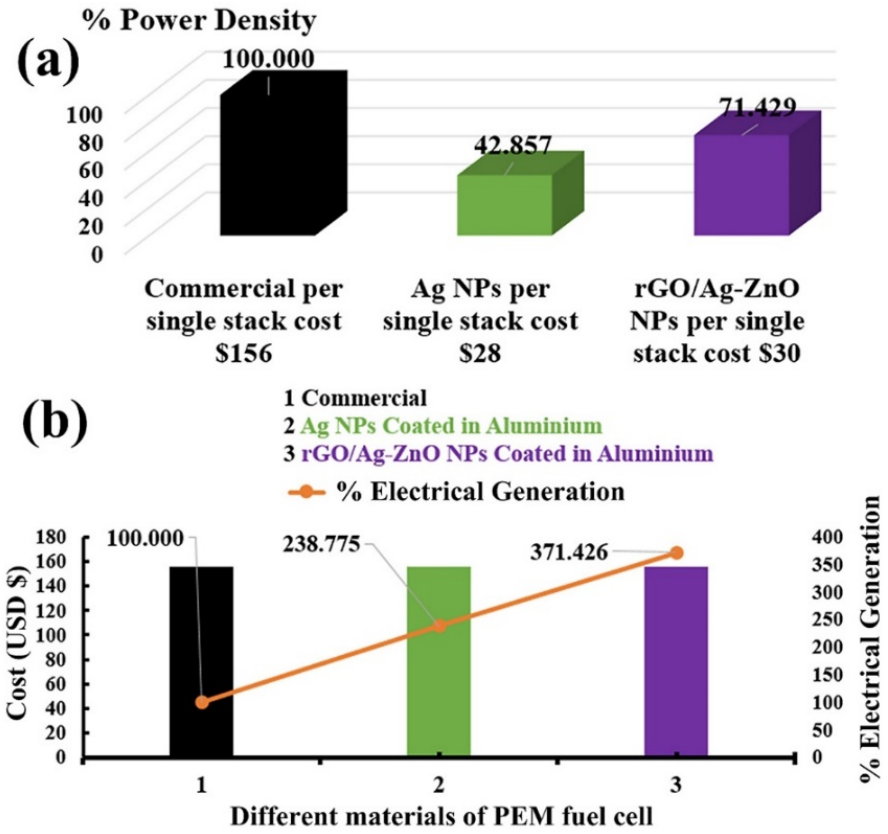

Figure 13 (a) Total cost vs percentage of power density generation, (b) Electricity production percentage by different PEM fuel cell after raising the cost level similar to the commercial PEM fuel cell.

Conclusions

Ag nanoparticles and rGO/Ag-ZnO nanomaterials were synthesised using eco-friendly *Callistemon viminalis* leaf extract. Scanning electron microscopy analysis for Ag nanoparticles showed an average size of 28 nm, XRD analysis crystal size of 22 nm (**Figure 9**), and TEM image analysis showed an average size of 46 nm conforming to a cubic shape (**Figure 8**). SEM image analysis for rGO/Ag-ZnO nanomaterials confirms the coating of reduced graphene oxide on silver composite zinc oxide nanomaterials (**Figure 4**(**a**)). XRD analysis showed Ag crystal size of 45 nm and ZnO crystal size of 22 nm (**Figure 9**) in rGO/Ag-ZnO nanomaterials. FTIR confirms the attachment of alcohol and carboxylic acid on the surface of both Ag nanomaterials and rGO/Ag-ZnO nanomaterials (**Figure 10**). A comparative study with a commercial PEM fuel cell and rGO/Ag-ZnO nanomaterials coatings on an aluminium plate showed similar power densities. The power density of Ag nanoparticle coatings on an aluminium plate was very low compared to the commercial PEM fuel cells and rGO/Ag-ZnO nanomaterials coated on an aluminium plate. This study shows that the presented eco-friendly method for nanomaterial synthesis are also capable of PEM fuel cell applications. In the context of enviro economic, silver nanoparticles coated aluminium electrode and rGO/Ag-ZnO nanomaterials are efficient enough to produce a comparatively higher percentage of electricity at a price of $156 than the commercial PEM fuel cell product and newly designed PEM fuel cell product, as shown in **Figure 13**(**b**).

Acknowledgements

The authors acknowledge the Thailand Graduate Institute of Science and Technology (TGIST), National Science and Technology Developmental Agency, Pathum Thani, Thailand, Agreement (No. SCA-CO-2562-9699-EN) for providing funding support to research student.

References

[1] NS Chaudhari, AP Bhirud, RS Sonawane, LK Nikam, SS Warule, VH Rane and BB Kale. Ecofriendly hydrogen production from abundant hydrogen sulfide using solar light-driven hierarchical nanostructured $ZnIn_2S_4$ photocatalyst. *Green Chem.* 2011; **13**, 2500-6.

[2] K Christmann, K Friedrich and N Zamel. Activation mechanisms in the catalyst coated membrane of PEM fuel cells. *Prog. Energ. Combust. Sci.* 2021; **85**, 100924.

[3] R Hanke-Rauschenbach, B Bensmann and P Millet. *Hydrogen production using high-pressure electrolyzers. In*: V Subramani, A Basile and TN Veziroğlu (Eds.). Compendium of hydrogen energy. Woodhead Publishing, Oxford, 2015, p. 179-224.

[4] J Joy, J Mathew and SC George. Nanomaterials for photoelectrochemical water splitting: Review. *Int. J. Hydrog. Energ.* 2018; **43**, 4804-17.

[5] K Jyoti, M Baunthiyal and A Singh. Characterization of silver nanoparticles synthesized using *Urtica dioica* Linn. leaves and their synergistic effects with antibiotics. *J. Radiat. Res. Appl. Sci*. 2016; **9**, 217-27.

[6] N Kilinc-Ata. Trends in the market growth for Proton Exchange Membrane Fuel Cell (PEMFC): A review of the literature and market dynamics. *Eur. J. Econ. Finance Adm. Sci.* 2007; **8**, 69-92.

[7] X Liu, X Li, X Liu, S He, J Jin and H Meng. Green preparation of Ag-ZnO-rGO nanoparticles for efficient adsorption and photodegradation activity. *Colloids Surf. A: Physicochem. Eng. Asp.* 2020; **584**, 124011.

[8] K Maeda and K Domen. Photocatalytic water splitting: Recent progress and future challenges. *J. Phys. Chem. Lett.* 2010; **1**, 2655-61.

[9] F Marques. Grand challenges in fuel cells: Materials issues at all length scales. *Front. Energ. Res.* 2013; **1**, 5.

[10] S Menon, H Agarwal, SR Kumar and SV Kumar. Green synthesis of silver nanoparticles using medicinal plant *Acalypha indica* leaf extracts and its application as an antioxidant and antimicrobial agent against foodborne pathogens. *Int. J. Appl. Pharm.* 2017; **9**, 42-50.

[11] YK Mohanta, SK Panda, AK Bastia and TK Mohanta. Biosynthesis of silver nanoparticles from *Protium serratum* and investigation of their potential impacts on food safety and control. *Front. Microbiol.* 2017; **8**, 626.

[12] PS Narayan, NL Teradal, S Jaldappagari and AK Satpati. Eco-friendly reduced graphene oxide for the determination of mycophenolate mofetil in pharmaceutical formulations. *J. Pharm. Anal.* 2018; **8**, 131-7.

[13] P Nikolaidis and A Poullikkas. A comparative overview of hydrogen production processes. *Renew. Sust. Energ. Rev.* 2017; **67**, 597-611.

[14] H Saleem, M Haneef and HY Abbasi. Synthesis route of reduced graphene oxide via thermal reduction of chemically exfoliated graphene oxide. *Mater. Chem. Phys.* 2017; **204**, 1-7.

[15] C Sealy. The problem with platinum. *Mater. Today* 2008; **11**, 65-8.

[16] A Shafaghat. Synthesis and characterization of silver nanoparticles by phytosynthesis method and their biological activity. *Synth. React. Inorg. Metal-Org. Nano-Met. Chem.* 2014; **45**, 381-7.

[17] N Singh, R Nyuur and B Richmond. Renewable energy development as a driver of economic growth: Evidence from multivariate panel data analysis. *Sustainability* 2019; **11**, 2418.

[18] T Taner. Alternative energy of the future: A technical note of PEM fuel cell water management. *J. Fundam. Renew. Energ. Appl.* 2015; **5**, 163.

[19] S Wi, H Woo, S Lee, J Kang, J Kim, S An, C Kim, S Nam, C Kim and B Park. Reduced graphene oxide/carbon double-coated 3-D porous ZnO aggregates as high-performance Li-ion anode materials. *Nanoscale Res. Lett.* 2015; **10**, 204.

[20] L Xin, Z Zhang, Z Wang, J Qi and W Li. Carbon supported Ag nanoparticles as high performance cathode catalyst for H2/O2 anion exchange membrane fuel cell. *Front. Chem.* 2013; **1**, 16.

[21] XH Yau, FW Low, CS Khe, CW Lai, SK Tiong and N Amin. An investigation of the stirring duration effect on synthesized graphene oxide for dye-sensitized solar cells. *PloS One* 2020; **15**, e0228322.

[22] QW Zhang, LG Lin and WC Ye. Techniques for extraction and isolation of natural products: A comprehensive review. *Chin. Med.* 2018; **13**, 20.

[23] PR Kumar, PL Suryawanshi, SP Gumfekar, BA Bhanvase and S Sonawane. Sonochemical synthesis of Pt-Co/C electrocatalyst for PEM fuel cell applications. *Surf. Interfaces* 2018; **12**, 116-23.

[24] AJ Hung, CC Yu, YH Chen and LY Sung. Cost analysis of proton exchange membrane fuel cell systems. *AIChE J.* 2008; **54**, 1798-810.